7th International Conference
on
Wind Turbine Noise
Rotterdam – 2nd to 5th May 2017

Use of the Acoustic Camera to accurately localise wind turbine noise sources and determine their Doppler shift

Stuart Bradley, Physics Department, University of Auckland, New Zealand: s.bradley@auckland.ac.nz

Michael Kerscher, gfaitech GmbH, Volmerstrasse 3, 12489 Berlin, Germany: kerscher@gfaitech.de

Torben Mikkelsen, Technical University of Denmark, Department of Wind Energy, Roskilde, Denmark: tomi@dtu.dk

Summary

The Acoustic Camera is frequently used to visualize the aero-acoustic noise from wind turbines, but 'ground truth' validation of accuracy has not generally been available. We describe an experiment in which eight small piezoelectric speakers were placed at positions along a turbine blade from near the hub to at the very tip, and on the leading and trailing edge of the blade. Six sources were attached on the suction (downwind) side of the blade, and two on the pressure (upwind) side. Each source generated a loud stable narrow-band tone. All sources were emitting simultaneously at slightly different frequencies. This multi-source configuration was recorded with a star-shaped 48-microphone Acoustic Camera of diameter 3.4 m, and a 120-microphone spiral array of diameter 4 m. Measurements were made with the turbine not rotating, as the turbine rotation speed increased, at full constant rotation speed, and as the turbine slowed down to stop. Cameras were placed on the ground downwind of the turbine along the turbine axis direction. Measurements were also conducted upwind of the turbine at hub height.

All eight sources were clearly identified even though they were close in frequency. The leading edge and trailing edge sources, which experienced very similar Doppler shift, were also clearly resolved. The location of each source predicted acoustically also agreed very closely with the location on the optical image obtained by the reference camera located at the centre of each microphone array. This was true even when the turbine was rotating at full speed.

The Doppler effects were dramatic, with the sources at varying radial distances along the blade experiencing different Doppler shift amplitudes. Particularly interesting effects will be described during speed up and slowing down of the turbine.

Overall, this experiment provides, for the first time, quantitative evidence of the source location accuracy of the Acoustic Camera for wind turbine noise estimation, as well as a quantitative assessment of the ability of the Acoustic Camera to characterise the time-dependent spectral changes along a blade due to Doppler shift.

1. Introduction

Wind turbines generate aero-acoustic noise from the blades which, because of periodicities, can cause annoyance at distances of hundreds of meters (Chen et al. 2016; Michaud et al, 2016; Dröes and Koster , 2016). The typical path length from turbine source to listener is such that meteorological influences are significant (Mittal et al. 2017; Gallo et al, 2016). In the absence of

very dense 3D meteorological measurements and an accompanying, *highly reliable*, sound propagation model, characterisation of the sources needs to be done close to the turbine. Measurements can be made on the blade itself (Bertagnolio et al, 2017), but this leaves a challenge to translate these measurements to what is heard in the far field. An alternative is to use a microphone array some tens of meters from the turbine, so that measurements are effectively far-field but close enough that intervening meteorological influences are not significant (Buck et al, 2016).

The Acoustic Camera is frequently used to visualize the aero acoustic noise from wind turbines, but 'ground truth' validation of accuracy has not generally been available. There are two main reasons why such validation is required. The first is that, because of the relatively slow speed of sound, the turbine rotates considerably during the emission of sound and its reception at the Acoustic Camera microphone array. This means that *registration* of the detected sound pattern on the blade requires assumptions about wind speed and direction, generally in addition to any wind vector measurements (Mo and Jiang, 2017; Zhang et al. 2017). The second reason that validation of Acoustic Camera data is required is that the sound from the blade undergoes huge Doppler shift due to the rapid rotation and the relatively close distance to the Acoustic Camera. Placing an Acoustic Camera further from the turbine will reduce Doppler shift, but also reduces the spatial resolution achieved by the Acoustic Camera and increases the uncertainties about meteorological effects.

Notwithstanding these difficulties, there is no doubt that Acoustic Camera images, such as that recorded by Oerlemans et al. (2007) and shown in Fig. 1, provide valuable insights into turbine noise generation, showing source location on the blade, spectral characteristics, and some measure of directionality, as the blade rotates.

Validation of Acoustic Camera methodology using the aero-acoustic noise generated by the turbine is not a realistic approach, because it is necessary to make an assumption about the sound which is being used for validation. For this reason, we have set up a *control experiment*, in which known sound sources are placed in known locations on a rotating turbine, and are then recorded and analysed using an Acoustic Camera.

2. Experimental Design

In this experiment, multiple small piezo-electric tonal sources were placed on one blade of an operational turbine, which was then allowed to rotate. Two models of Acoustic Camera arrays were used to make measurements of the sound received 50 m from the turbine.

2.1 Acoustic Sources

Eight small piezoelectric speakers were placed at positions along a turbine blade from near the hub to at the very tip, and on the leading and trailing edge of the blade. Six sources were attached on the suction (downwind) side of the blade, and two on the pressure (upwind) side. Each source generated a loud stable narrow-band tone. All sources were emitting simultaneously at slightly different frequencies. The sources, each weighing 55 g, were each powered by a light battery (the dominant weight) and taped to the blade at measured locations as shown in Fig. 2.

The tone frequencies, in ascending order, are 3068, 3069, 3090, 3101, 3308, 3405, 3409, and 3453 Hz for sources 4, 5, 2, 3, 1, 7, 8, and 6 respectively. The variation is due to the manufacturer’s tolerance for these inexpensive piezo buzzers. Note that sources 4 and 5 are very close in frequency, as are sources 1 and 7 on the tip.

2.2 Acoustic Camera

This multi-source configuration was recorded with a star-shaped 48-microphone Acoustic Camera of diameter 3.4 m (a Star48), and a 120-microphone spiral array of diameter 4 m (a FlexStar120). The Acoustic Cameras were placed on the ground 48.5 m downwind of the turbine along the turbine axis direction, as shown in Fig. 3. Measurements were also conducted upwind of the turbine at hub height using the Star48 from a hoist.

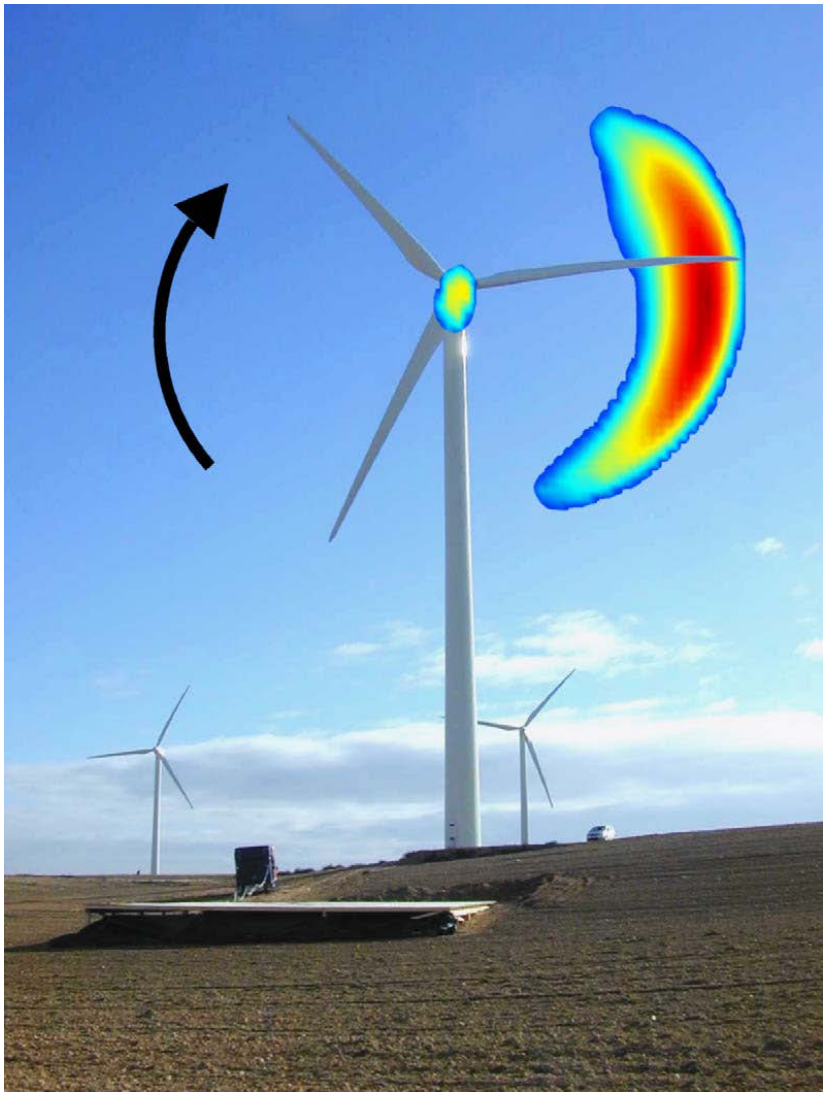

Figure 1. Use of an array of microphones to image turbine noise sources (from by Oerlemans et al. 2007) .

2.3 Turbine Operation

The sources were mounted on a Nordtank NTK 500/41 500 kW turbine of diameter 41 m, swept area 1325 m², a maximum rotor speed of 27 rpm, a tip speed of 58 m/s, and hub height 50 m. Measurements were made with the turbine not rotating, as the turbine rotation speed increased, at full constant rotation speed, and as the turbine slowed down to stop. The turbine has an air-brake by turning the tip of one of the blades by 90°, as seen on the left in Fig. 2.

3. Location of Sources

Fig. 4 shows Acoustic Camera resolution of sources on the blade face which is toward the Star 48 using a spectral filter which encompasses all sources (the turbine is static) Sources 3 and 4 show as a double-sized contour, and are not quite individually resolved. Fig. 5 shows source location based on tighter bandwidth filters (as indicated on the figure).

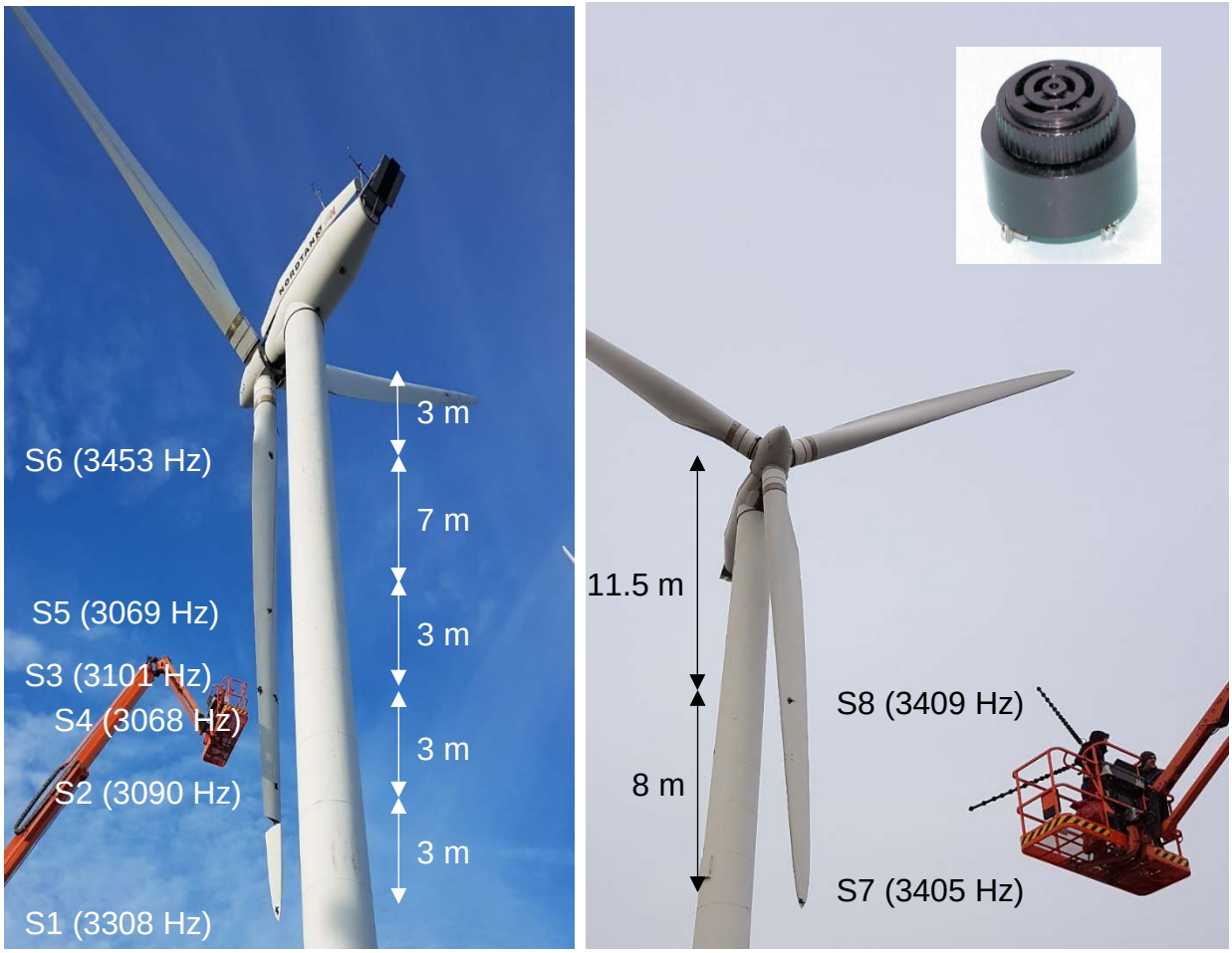

Figure 2. The location and tone frequency of the 8 speakers. Inset: one of the speakers.

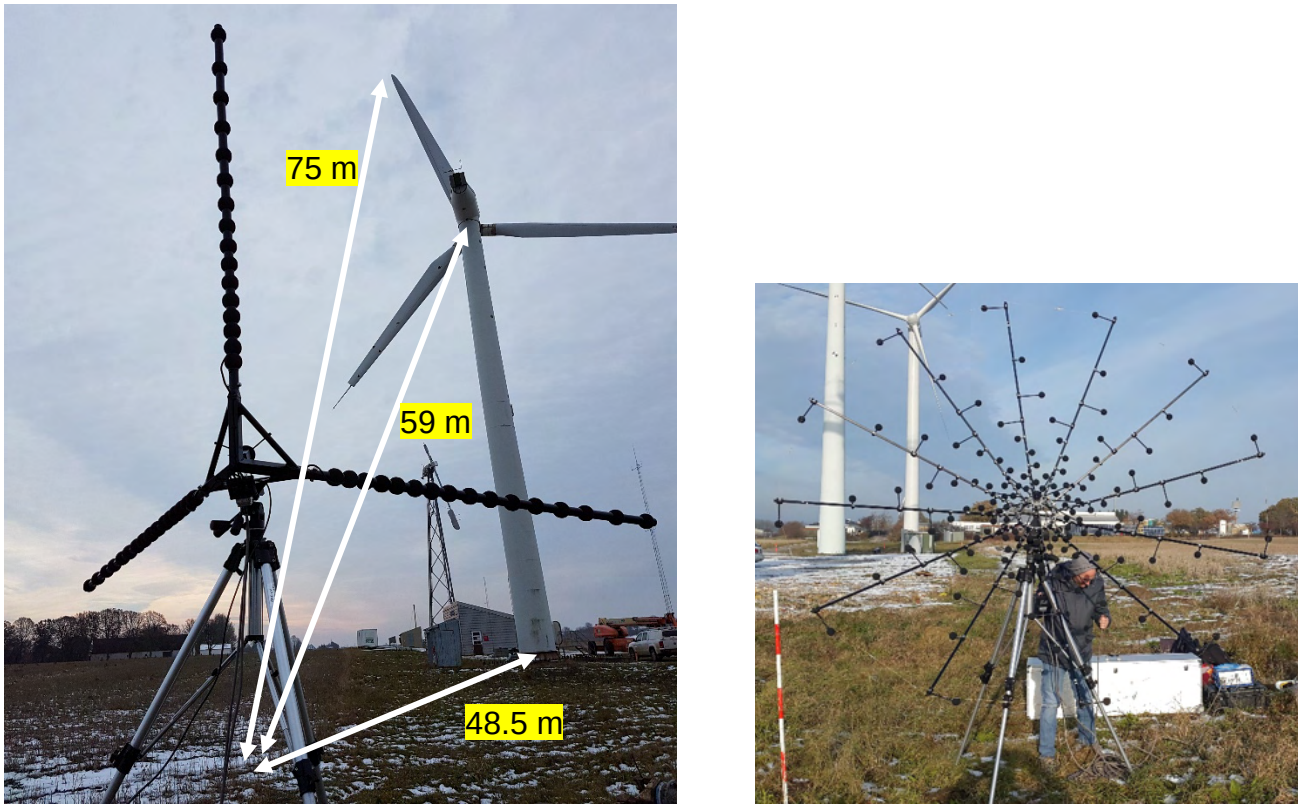

Figure 3. The turbine and Star48 array (left), and the FlexStar120 (right).

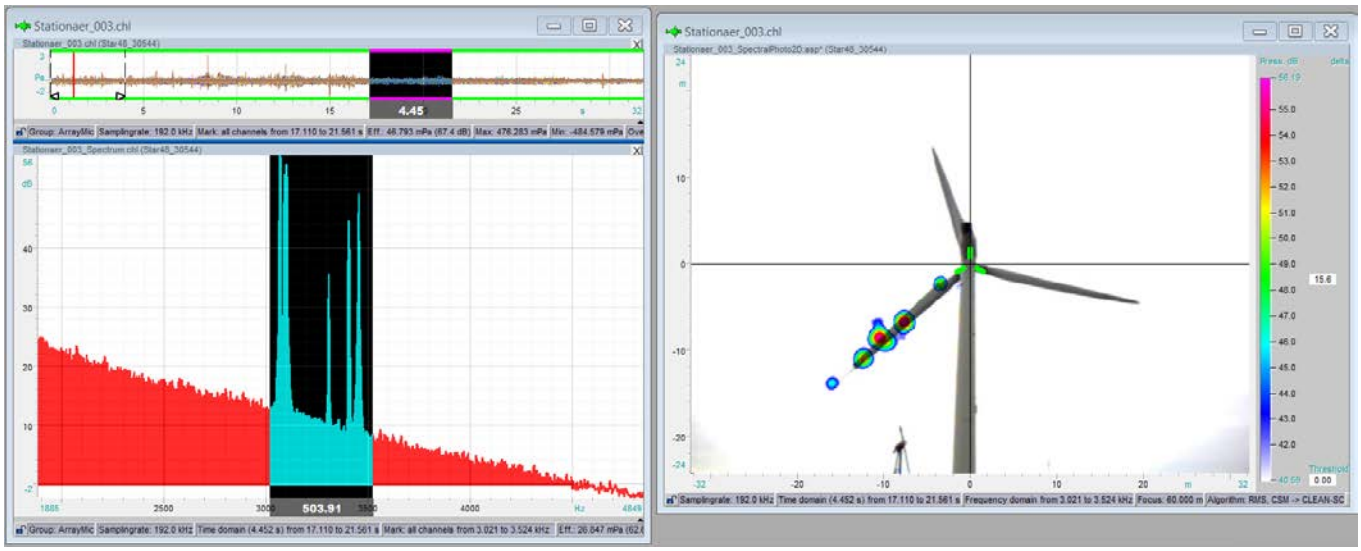

Figure 4. Time record (top, spectrum (left) and sources (right) for the static turbine (Star48).

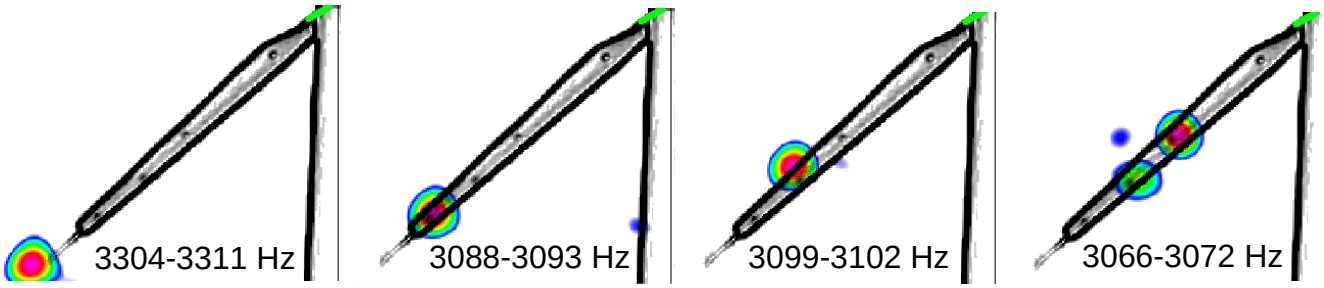

Figure 5. Source location using Star48.

The tighter bandwidth allows source 3 to be clearly separated from the nearby source 4. The rightmost of these frames shows sources 4 and 5 clearly resolved (they are spatially well separated but have frequencies within 1 Hz). In three of these frames minor reflections can also be seen, possibly from the tower, giving a spurious blue-coloured point. Similar results are obtained for source 6.

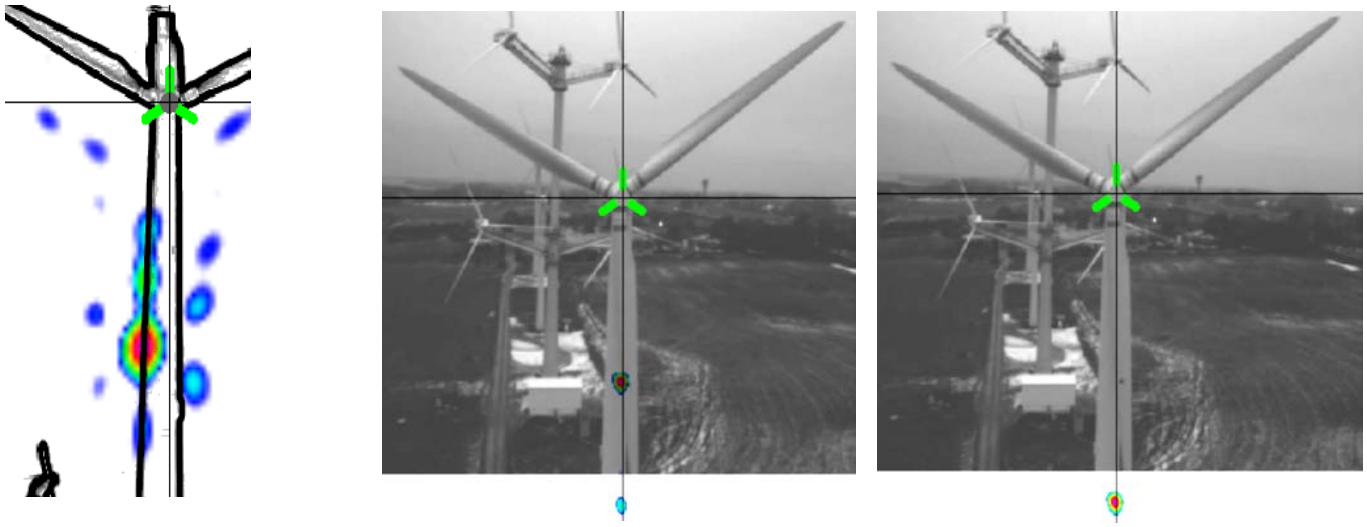

Figure 6. FlexStar120 image with the turbine rotating at constant speed (left), and Star48 images from the hoist at hub height with filters for source 8 (centre) and 7 (right).

When the turbine is fully rotating at constant speed, source location appears to be not nearly as good (left frame, Fig. 6). Three of the sources are resolved and possibly with further frequency selection 4 could be resolved. It may be possible here that the bandwidth chosen did reflect the Doppler shifts fully, and more work needs to be done on that (this figure was obtained in a 'quick look' at the data, immediately after the experiment). There are also spurious 'sources' from reflections, most likely off the tower.
Measurements were also made of the sources on the upwind face of the blade (also in Fig. 6) when the turbine was static, with similar results to those for the downwind face.

4. Doppler Shift

The Doppler shift is captured in Fig. 7 as the turbine speeds up from rest. The entire 8 sources can be identified, although the two on the blade face away from the Acoustic camera have much lower amplitude. In Fig. 7, from the top down, sources are 6, 7 and 8 (fainter), 1, 3 and 2, and 4 and 5. The relative amplitudes of the frequency variation are expected to increase with radial distance from the hub in the order 6, 5, 8, 3 and 4, 2, 1 and 7. It is difficult to separate those sources which are close in frequency, but it is clear that source 6 has the smallest FM amplitude and sources 1 and 7 have the highest amplitude.

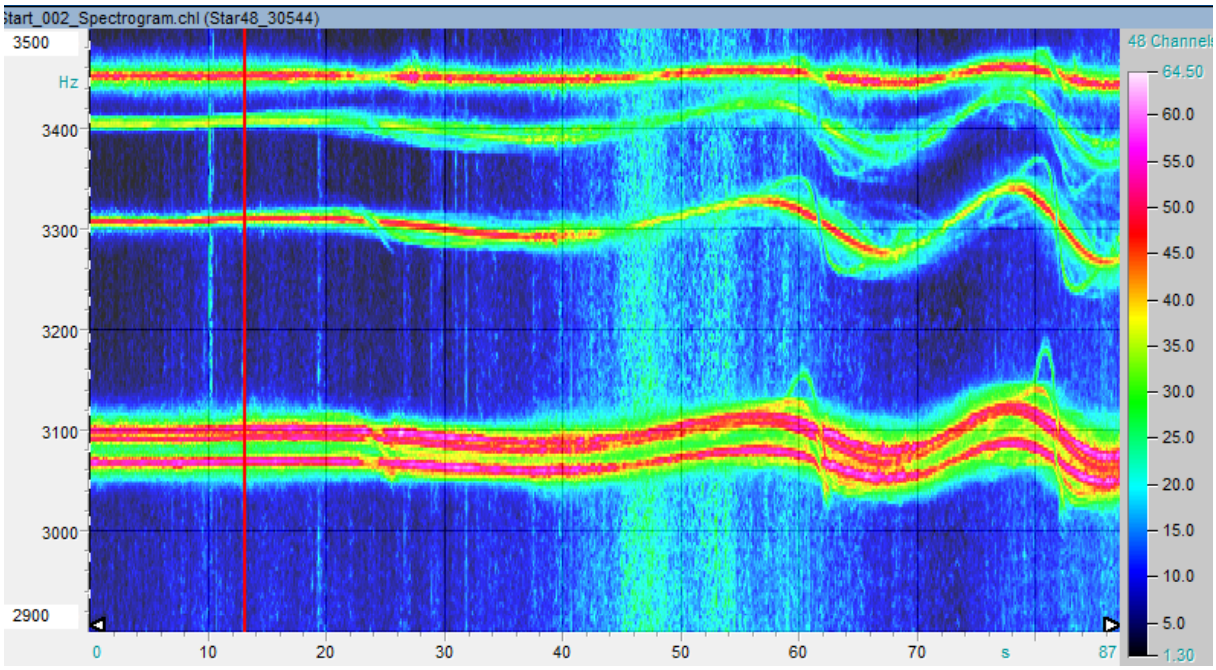

Figure 8.Doppler shift commencing as the turbine spins up.

Sequences are shown in Fig. 9 at constant turbine rotation and as the turbine slows down to stop.

5. Conclusions

Overall, this experiment provides, for the first time, quantitative evidence of the source location accuracy of the Acoustic Camera for wind turbine noise estimation, as well as a quantitative assessment of the ability of the Acoustic Camera to characterise the time-dependent spectral changes along a blade due to Doppler shift. The ability of an Acoustic Camera to localise individual point tonal 3 kHz sources is exceptional! In Fig. 10 the optical and acoustic source separation is compared with a 1 m circle, showing that the acoustic spatial resolution is around ½ m.

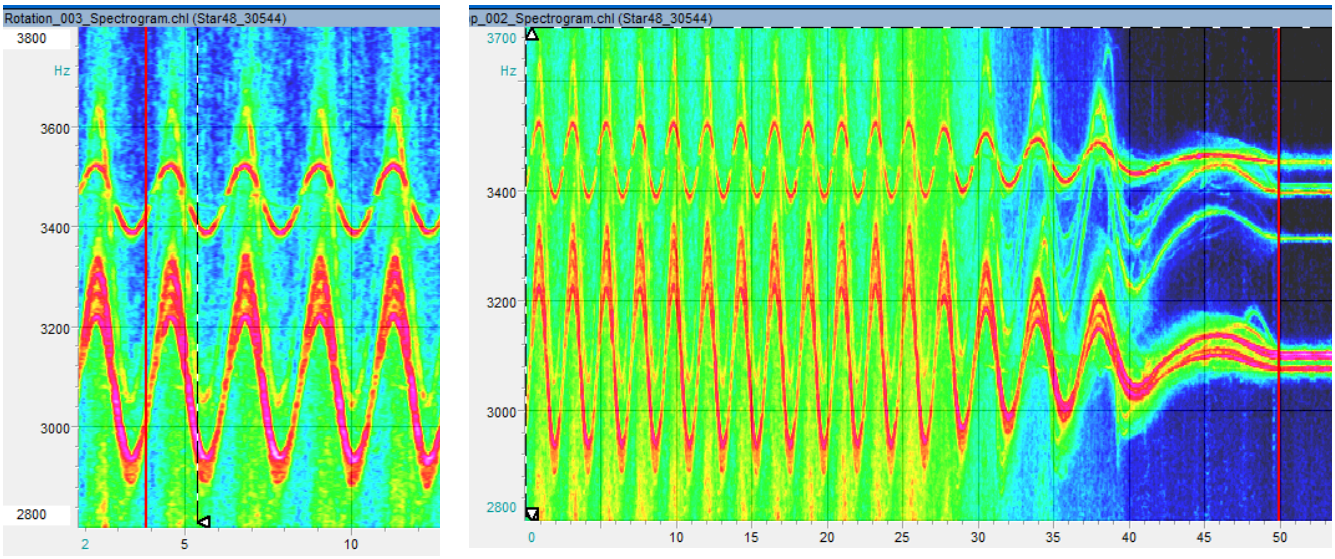

Figure 9. Doppler shift at constant rotation (left) and as the turbine slows down (right) for selected sources.

This work gives confidence in the current ability of Acoustic Cameras to adequately register sources with sufficient precision, and also to measure the Doppler shift as a function of radial distance (i.e. as a function of speed of the sources). This should allow the Doppler effects to be removed so that true source characterisation can be obtained.

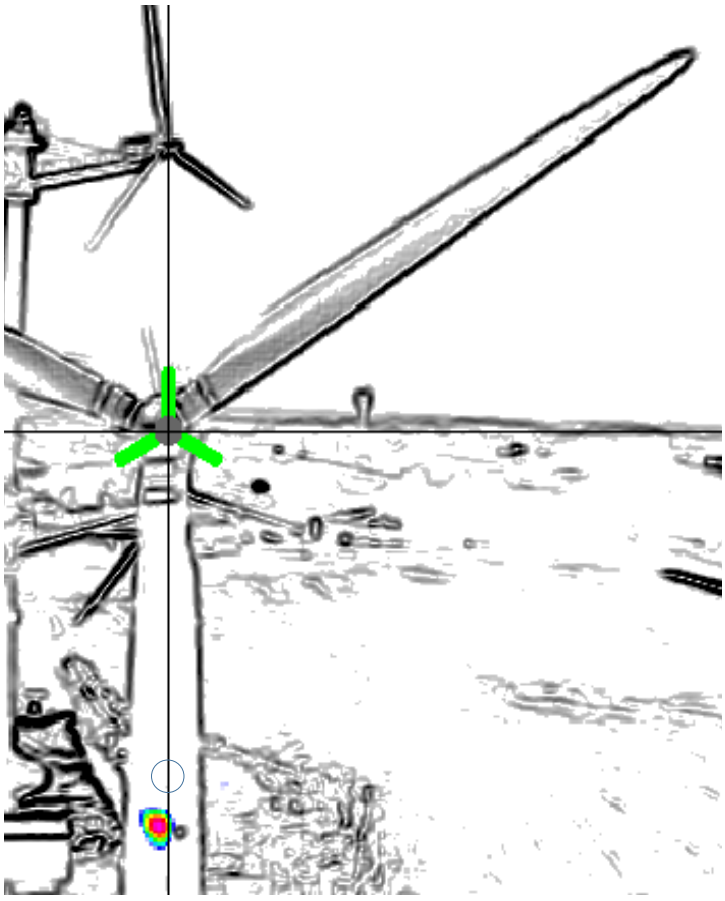

Figure 10. An Acoustic camera optical image with edge detection, showing one of the sources, together with the acoustic source location. Just above this point is drawn a 1 m – dimeter circle.

References

Bertagnolio F, Madsen H A, Fischer A and Bak C (2017) *A semi-empirical airfoil stall noise model based on surface pressure measurements*. J Sound Vibration 387, 127–162.

Bower, T, Villeneuve, P J, Russell, E, Koren, G, and van Den Berg, F (2016) *Self-reported and measured stress related responses associated with exposure to wind turbine noise.* JASA 139(3), 1467-1479.

Buck S, Oerlemans S. and Palo S (2016) *Experimental characterization of turbulent inflow noise on a full-scale wind turbine*. J Sound Vibration 385, 219–238.

Chen L, Harding C, Sharma A and MacDonald E (2016). *Modeling noise and lease soft costs improves wind farm design and cost-of-energy predictions.* Renewable Energy, 97, 849-859.

Dröes M I and Koster H R A (2016). *Renewable energy and negative externalities: The effect of wind turbines on house prices.* J Urb Econ, 96, 121–141.

Michaud, D S; Feder, K, Keith, S E, Voicescu, S A, Marro, L, Than, J, Guay, M, Denning, A, Gallo, P, Fredianelli, L, Palazzuoli, D, Licitra, G and Fidecaro F (2016) *A procedure for the assessment of wind turbine noise.* Appl Acoustics 114, 213–217.

Mittal P, Mitra K, and Kulkarni K (2017). *Optimizing the number and locations of turbines in a wind farm addressing energy-noise trade-off: A hybrid approach.* Energy Conversion and Management, 132 147–160.

Mo P, and Jiang W (2017) *A hybrid deconvolution approach to separate static and moving single-tone acoustic sources by phased microphone array measurements.* Mech Systems Sig Proc 84, 399–413.

Oerlemans, S, Sijtsma, P and Méndez López B (2007) *Location and quantification of noise sources on a wind turbine*. J Sound Vibration 299, 869-883.

Zhang X-Z, Bi C-X, Zhang Y-B and Xu L (2017). *A time-domain inverse technique for the localization and quantification of rotating sound sources.* Mech Systems Sig Proc 90,15–29.